Dyrk1A negatively regulates the actin cytoskeleton through threonine phosphorylation of N-WASP

Joongkyu Park[1], Jee Young Sung[1,*], Joohyun Park[2], Woo-Joo Song[3], Sunghoe Chang[2] and Kwang Chul Chung[1,‡]

[1]Department of Systems Biology, College of Life Science and Biotechnology, Yonsei University, Seoul 120–749, Republic of Korea
[2]Department of Biomedical Sciences, Seoul National University, College of Medicine, Seoul 110–799, Republic of Korea
[3]Graduate Program in Neuroscience, Institute for Brain Science and Technology, FIRST Research Group, Inje University, Busan 633-146, Republic of Korea

*Present address: Division of Specific Organs Cancer, Pediatric Oncology Division, National Cancer Center, Goyang-si, Gyeonggi-Province 410-769, Republic of Korea
‡Author for correspondence (kchung@yonsei.ac.kr)

Accepted 22 August 2011
Journal of Cell Science 125, 67–80

doi: 10.1242/jcs.086124

Summary

Neural Wiskott–Aldrich syndrome protein (N-WASP) is involved in tight regulation of actin polymerization and dynamics. N-WASP activity is regulated by intramolecular interaction, binding to small GTPases and tyrosine phosphorylation. Here, we report on a novel regulatory mechanism; we demonstrate that N-WASP interacts with dual-specificity tyrosine-phosphorylation-regulated kinase 1A (Dyrk1A). In vitro kinase assays indicate that Dyrk1A directly phosphorylates the GTPase-binding domain (GBD) of N-WASP at three sites (Thr196, Thr202 and Thr259). Phosphorylation of the GBD by Dyrk1A promotes the intramolecular interaction of the GBD and verprolin, cofilin and acidic (VCA) domains of N-WASP, and subsequently inhibits Arp2/3-complex-mediated actin polymerization. Overexpression of either Dyrk1A or a phospho-mimetic N-WASP mutant inhibits filopodia formation in COS-7 cells. By contrast, the knockdown of Dyrk1A expression or overexpression of a phospho-deficient N-WASP mutant promotes filopodia formation. Furthermore, the overexpression of a phospho-mimetic N-WASP mutant significantly inhibits dendritic spine formation in primary hippocampal neurons. These findings suggest that Dyrk1A negatively regulates actin filament assembly by phosphorylating N-WASP, which ultimately promotes the intramolecular interaction of its GBD and VCA domains. These results provide insight on the mechanisms contributing to diverse actin-based cellular processes such as cell migration, endocytosis and neuronal differentiation.

Key words: N-WASP, Phosphorylation, Dyrk1A, Actin cytoskeleton, Filopodia, Dendritic spine

Introduction

Actin polymerization and dynamics are involved in diverse cellular processes including cell migration, morphogenesis, endocytosis, vesicle trafficking and phagocytosis (Mattila and Lappalainen, 2008). The coordinated assembly of actin filaments adjacent to cell membranes results in the formation of distinct cellular structures called filopodia, lamellipodia and dendritic spines (Goley and Welch, 2006; Mattila and Lappalainen, 2008). Actin polymerization is tightly regulated by various proteins, such as phosphoinositides, membrane-bound small G-proteins, Wiskott–Aldrich syndrome protein (WASP) family members and actin-related protein (Arp) 2/3 (Takenawa and Suetsugu, 2007). Neural-WASP (N-WASP) is abundantly expressed by neural tissues and plays a critical role in the formation and regulation of actin filament assembly (Takenawa and Suetsugu, 2007).

N-WASP activity is regulated by a multitude of factors. For example, the binding of N-WASP to phosphoinositides through its basic domain or small GTPases through its GTPase-binding domain (GBD) stimulates actin polymerization (Rohatgi et al., 2000). In addition, the C-terminal verprolin, cofilin and acidic (VCA) domain of N-WASP interacts with actin monomers and Arp2/3 to initiate actin polymerization (Machesky and Insall, 1998). The intramolecular interaction between GBD and VCA results in the folding of the N-WASP protein molecule, which inhibits its function (Kim et al., 2000; Prehoda et al., 2000). Furthermore, N-WASP is modified and regulated by protein phosphorylation. Src-kinase-mediated tyrosine phosphorylation within the GBD activates N-WASP, which subsequently stimulates neurite extension (Suetsugu et al., 2002). To date, several studies have demonstrated phosphorylation of tyrosine and/or serine residues within the GBD or VCA domain of WASP; however, the precise in vivo functions of these phosphorylation events have not been clearly elucidated (Dovas and Cox, 2010).

Dual-specificity tyrosine-phosphorylation-regulated kinase 1A (Dyrk1A) is a proline-directed serine/threonine kinase (Himpel et al., 2000). Dyrk1A interacts with more than 20 substrates involved in various cellular processes including cell cycle control, synaptic function, vertebrate development and neurodegeneration (Park et al., 2009a). More importantly, the abnormal accumulation of Dyrk1A is closely associated with the presence of neural defects observed in patients with Down syndrome (DS) (Park et al., 2009b). Interestingly, several reports implicate a biochemical and functional link between Dyrk1A and N-WASP. For example, these two proteins share the same binding partners, such as dynamin-1, amphiphysin-1 and synaptojanin-1 (Adayev et al., 2006; Chen-Hwang et al., 2002; Murakami et al., 2006; Shin et al., 2007; Yamada et al., 2009). In addition, yeast Pom1 and *Drosophila* minibrain (MNB) kinases, which are homologs of the Dyrk family proteins, have been reported to be involved in regulation of actin cytoskeleton (Liu

et al, 2009; Tatebe et al, 2008). The relationship between Dyrk1A and N-WASP and the contribution of Dyrk1A to actin filament assembly have not been fully elucidated.

Here, we demonstrate that Dyrk1A directly phosphorylates N-WASP and promotes the intramolecular interaction of its GBD and VCA domains, which subsequently inhibits Arp2/3-mediated actin polymerization. This molecular sequence of events negatively regulates actin filament assembly.

Results

Dyrk1A binds to N-WASP

Based on the speculation that Dyrk1A might be functionally linked to N-WASP and/or its upstream or downstream signaling pathway components, we first assessed whether Dyrk1A interacts with N-WASP. HEK293 cells were co-transfected with plasmids encoding Xpress-tagged rat Dyrk1A and FLAG-tagged rat N-WASP, and the total cell lysates were immunoprecipitated with anti-FLAG antibody. Immunoblot analysis of anti-FLAG immunoprecipitates with anti-Xpress antibody revealed an interaction between ectopically expressed Dyrk1A and N-WASP (Fig. 1A). To determine whether these proteins directly bind to each other, bacterially expressed and purified recombinant Dyrk1A and N-WASP proteins were mixed and incubated in vitro. The samples were immunoprecipitated with anti-Dyrk1A antibody. Immunoblot analysis of anti-Dyrk1A immunocomplexes with anti-N-WASP antibody showed that these proteins directly interact (Fig. 1B). To examine whether the Dyrk1A–N-WASP interaction also occurs in vivo in tissues, such as the hippocampus, we performed co-immunoprecipitation assays on hippocampal lysates from embryonic day (E) 18 Sprague–Dawley rats. As shown in Fig. 1C, immunoblot analysis of anti-N-WASP immunoprecipitates using anti-Dyrk1A antibody confirmed that Dyrk1A and N-WASP interact in the hippocampus of embryonic rats. These results demonstrate that Dyrk1A binds to N-WASP in vitro and in vivo.

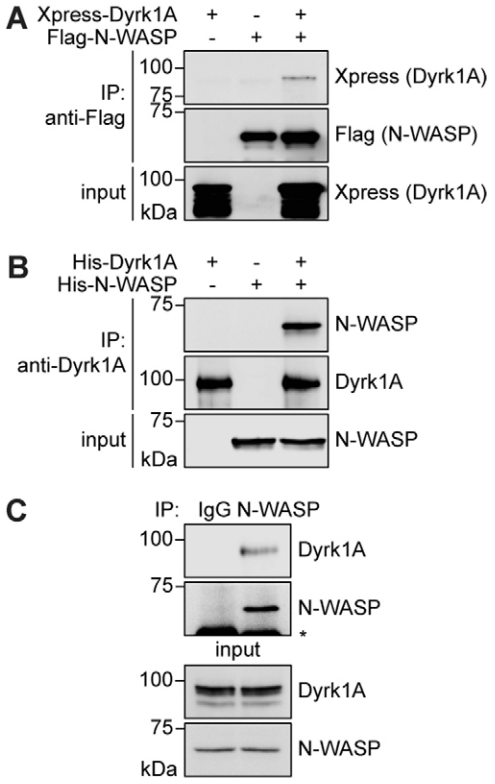

Fig. 1. Dyrk1A interacts with N-WASP. (**A**) Co-immunoprecipitation and immunoblotting analysis of the interaction between Xpress-tagged Dyrk1A and FLAG-tagged N-WASP in HEK293 cells. Proper expression of the transiently expressed Dyrk1A was verified by immunoblotting analysis with anti-Xpress antibody. (**B**) In vitro binding test between bacterial recombinant Dyrk1A and N-WASP. The purified Dyrk1A and N-WASP proteins were incubated overnight at 4℃, and the protein complexes were immunoprecipitated with anti-Dyrk1A antibody. (**C**) Co-immunoprecipitation and immunoblot analysis of the interaction between endogenous Dyrk1A and N-WASP in hippocampal lysates from E18.5 rat brains. The asterisk indicates the immunoglobulin G heavy chains.

Dyrk1A directly phosphorylates the GTPase-binding domain of N-WASP

To address whether Dyrk1A directly phosphorylates N-WASP, an in vitro kinase assay was performed using anti-Xpress immunoprecipitates (express Dyrk1A) from HEK293 cell lysates and bacterial recombinant 6×His-tagged N-WASP. Autoradiographic analysis of the reaction products demonstrated that Dyrk1A directly phosphorylates N-WASP in vitro (Fig. 2A). To exclude the possibility that N-WASP phosphorylation results from the action of an unidentified protein contaminant in the cell lysates, we used bacterially recombinant Dyrk1A. As shown in Fig. 2B, there was a clear band corresponding to N-WASP in the presence of recombinant Dyrk1A in vitro. These results demonstrate that Dyrk1A directly phosphorylates N-WASP. To specifically locate the region of N-WASP phosphorylated by Dyrk1A, the kinase assays were performed with various N-WASP truncation mutants. Among the tested mutants, the N-WASP(1–463), N-WASP(1–391) and N-WASP(1–264) mutants were phosphorylated by Dyrk1A to a similar extent as full-length N-WASP. However, N-WASP(1–195), the mutant lacking a GTPase-binding domain (GBD), was not phosphorylated by Dyrk1A (Fig. 2B,C). These data indicate that Dyrk1A phosphorylates the GBD of N-WASP, which spans amino acids 196–264.

To identify the exact phosphorylation site(s) on N-WASP (196-294), we generated N-WASP mutants having alanine substitutions at serine (Ser) and threonine (Thr) residues within the GBD based on the findings that Dyrk1A phosphorylates Ser or Thr residues of a substrate (Himpel et al., 2000; Lochhead et al., 2005) and Dyrk1A overexpression caused no significant change in tyrosine phosphorylation of N-WASP (supplementary material Fig. S1). There are three serine and five threonine residues within the GBD. We successfully generated seven N-WASP mutants having a point mutation at Thr196, Thr202, Ser204, Thr218, Thr248, Ser249 and Thr259. Unfortunately, an N-WASP mutant protein with a Ser239Ala substitution could not be generated because of technical difficulties. We then performed an in vitro kinase assay using recombinant Dyrk1A and each point mutant as the substrate. As shown in Fig. 2D, several N-WASP mutants having alanine mutations at Thr196, Thr202, Ser204 and Thr259 exhibited an obvious reduction in Dyrk1A-mediated phosphorylation, whereas the other N-WASP mutants had little to no effect on phosphorylation. Furthermore, the N-WASP mutant with triple alanine substitutions at Thr196, Thr202 and Thr259 experienced a greater than 80% reduction in Dyrk1A phosphorylation compared with WT N-WASP (Fig. 2E). Overall, these data indicate that Dyrk1A mainly phosphorylates N-WASP within the GBD at Thr196, Thr202 and Thr259.

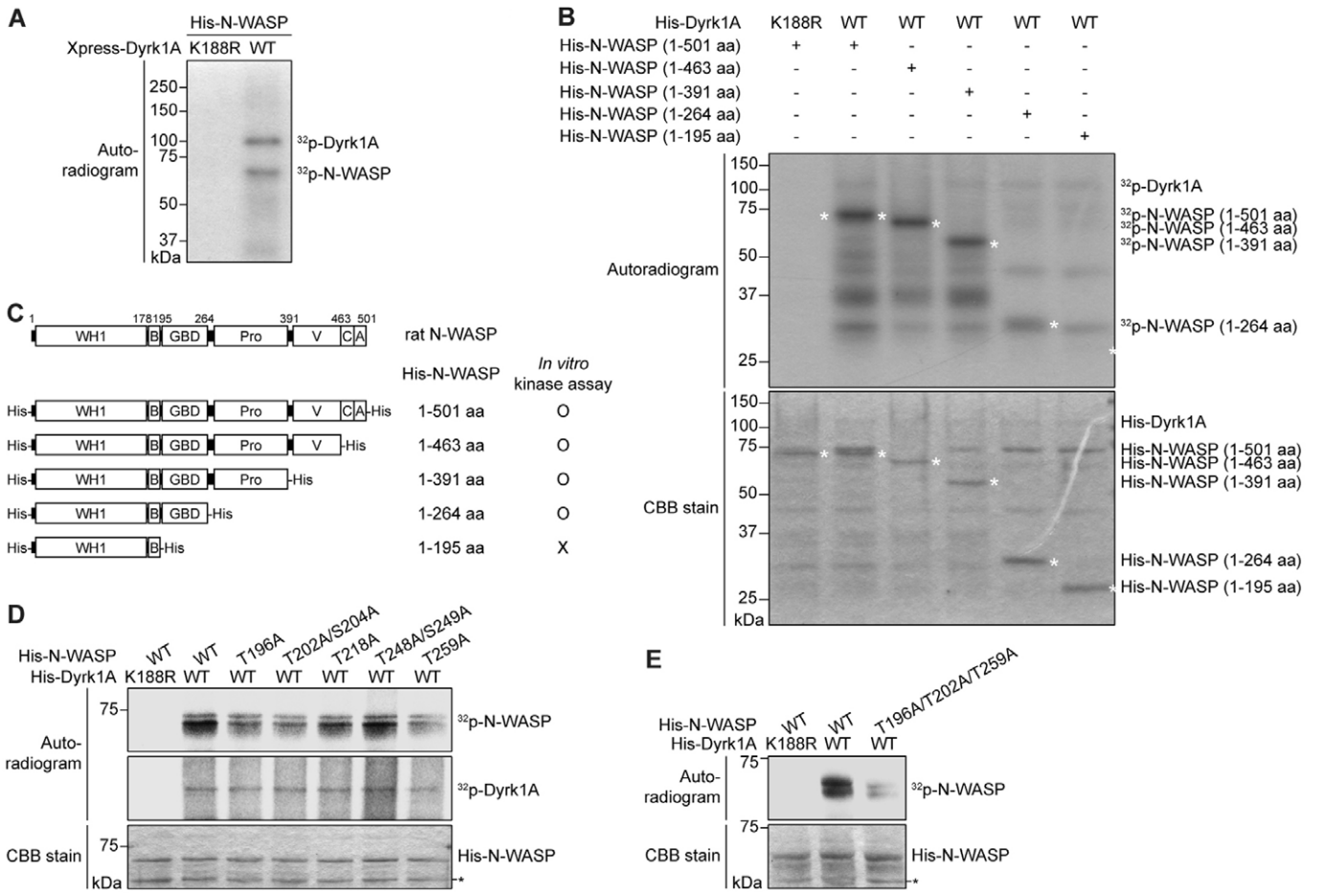

Fig. 2. Dyrk1A directly phosphorylates the GTPase-binding domain of N-WASP. (**A**) In vitro kinase assay with Dyrk1A using N-WASP as a substrate. Anti-Dyrk1A-immunocomplexes prepared from HEK293 cell lysates containing Xpress-tagged WT or kinase-inactive (K188R) Dyrk1A were incubated with recombinant 6 × His-tagged N-WASP and [γ-^{32}P]ATP. The reaction products were separated by SDS-PAGE. (**B**,**C**) Identification of Dyrk1A-targeting domain(s) within the N-WASP protein. In vitro kinase assays were performed using several bacterial recombinant and purified truncation mutants of N-WASP as indicated. The asterisks indicate the locations of N-WASP truncation mutant proteins (B). Schematic representation of N-WASP WT and truncation mutants, and summary of the results from an in vitro Dyrk1A phosphorylation assay with those mutants (C). N-WASP contains a WASP homology 1 domain (WH1), basic domain (B), GTPase-binding domain (GBD), proline-rich domain (Pro), and verprolin–cofilin–acidic domain (VCA). Note that Dyrk1A phosphorylates the GBD of N-WASP, which spans amino acids 196–264. (**D**,**E**) Identification of Dyrk1A-mediated phosphorylation site(s) within the N-WASP-GBD. An in vitro kinase assay was performed by incubating purified 6 × His-tagged Dyrk1A WT or K188R protein, recombinant 6 × His-tagged N-WASP WT or alanine substitution mutants and [γ-^{32}P]ATP. The asterisk indicates non-specific proteins. Note that the triple alanine substitution at Thr196, Thr202 and Thr259 almost failed to be phosphorylated by Dyrk1A (E).

Dyrk1A-mediated phosphorylation of N-WASP within the GBD does not affect the binding affinity of N-WASP to Cdc42

We assessed the functional effect of Dyrk1A-induced phosphorylation on N-WASP activity. The GTPase-binding domain of N-WASP interacts with the upstream small GTPase Cdc42 (Aspenstrom et al., 1996). Binding to Cdc42 alters the protein structure of N-WASP; this activates downstream Arp2/3-mediated signaling, which subsequently leads to the assembly of actin filaments (Mattila and Lappalainen, 2008). We first examined whether Dyrk1A phosphorylation affects the binding affinity of N-WASP for Cdc42. HEK293 cells were co-transfected with plasmids encoding constitutively active Cdc42 (V12) fused to GST and a FLAG-tagged N-WASP mutant, which has a glutamate substitution at the target Thr residue(s), which mimics the effect of Dyrk1A-mediated phosphorylations on N-WASP. Immunoblot analysis of the pull-down precipitates with anti-FLAG antibody showed that three N-WASP proteins with a single phosphorylation (T196E, T202E and T259E) do not differentially bind to Cdc42, compared with WT N-WASP (Fig. 3A). To examine the cooperative effects of the multiple phosphorylations, we performed additional co-immunoprecipitation assays using the mutants with either double substitutions at close T196E and T202E residues or triple substitutions at T196E,T202E,T259E (3TE). As shown in Fig. 3B, the binding of these two mutants with double or triple glutamate substitutions to Cdc42 was unaffected. To exclude the possibility of binding effects by unidentified endogenous proteins, we additionally tested in vitro binding of either bacterially purified WT N-WASP or 3TE mutant to purified Cdc42 (V12) from HEK293 cell lysates. Immunoblot analysis of the pull-down precipitates with anti-His antibody confirmed that the binding of N-WASP to Cdc42 is not affected by Dyrk1A

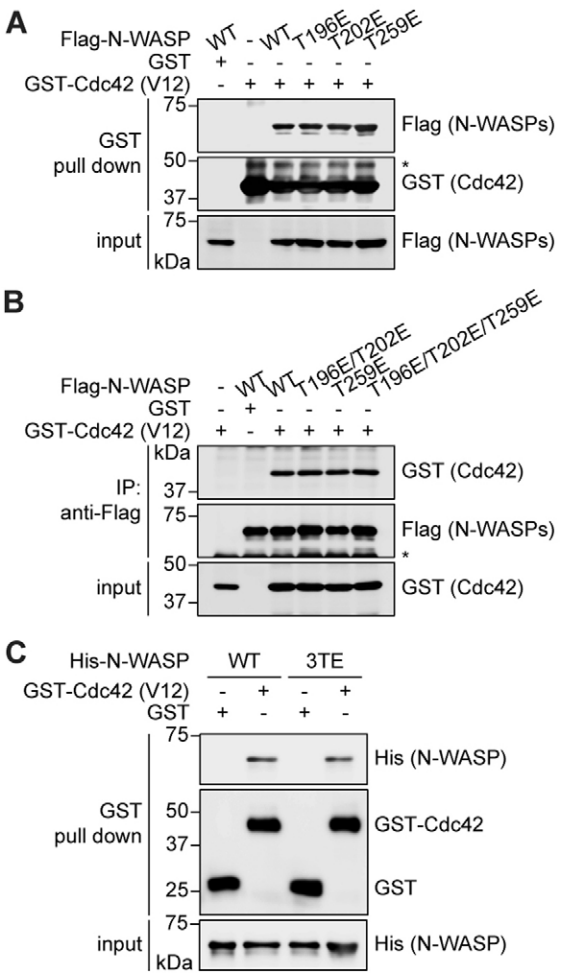

Fig. 3. Dyrk1A-induced phosphorylation of the GBD does not change the binding affinity of N-WASP for Cdc42. (**A**,**B**) Co-immunoprecipitation and immunoblot analysis of the interaction between GST-fused constitutively active Cdc42 (V12) and FLAG-tagged N-WASP phosphorylation-mimic single (A), and double and triple (B) glutamate mutations. Note that the phospho-mimetic mutation had no effect on the binding affinity of N-WASP to Cdc42. The asterisks indicate the immunoglobulin G heavy chains. (**C**) In vitro binding test between recombinant His-tagged N-WASP (WT or 3TE) and purified GST-fused Cdc42 (V12) from HEK293 cell lysates. The purified N-WASP and Cdc42 proteins were incubated with glutathione-Sepharose beads at 4℃ overnight, and the protein complexes were pulled down and subjected to immunoblotting analysis with anti-His antibody.

phosphorylation within the GBD (Fig. 3C). These data indicate that Dyrk1A-mediated phosphorylation of the GBD does not affect the binding affinity of N-WASP for Cdc42.

GBD phosphorylation regulates the intramolecular interaction of N-WASP domains and Arp2/3-mediated actin polymerization

In addition to the upstream Cdc42 protein, the GBD of N-WASP binds to the C-terminal verprolin, cofilin, acidic (VCA) domain through an intramolecular interaction (Prehoda et al., 2000). To examine whether Dyrk1A-mediated phosphorylation on the N-WASP GBD region alters this intramolecular interaction, co-immunoprecipitation followed by immunoblot analysis of HEK293 cell lysates prepared after transient transfection with the FLAG-tagged N-WASP fragment expressing the basic domain (B) plus GBD and Xpress-tagged VCA fragment were performed (Fig. 4A). As shown in Fig. 4B–D, glutamate substitution at Thr259 (T259E) resulted in a significant 2.8-fold increase in the interaction of B-GBD with the VCA domain, compared with the same interactions in WT N-WASP ($P<0.05$), whereas the substitution at Thr196 and Thr202 (T196E and T202E) had no significant effect ($P>0.05$). We speculate that the phosphorylation at Thr259 mainly contributes to the Dyrk1A-induced binding of the GBD of N-WASP to the VCA domain. This hypothesis is further supported by additional co-immunoprecipitation studies using an alanine substitution mutant at Thr259 (T259A). As shown in Fig. 4C,D, the phospho-mimetic T259E N-WASP mutant exhibited an increase in its intramolecular interaction, whereas the phospho-deficient T259A mutant exhibited no significant increase, compared with the WT N-WASP GBD ($P>0.05$). These results strongly indicate that Dyrk1A-mediated Thr259 phosphorylation promotes intramolecular interaction between the GBD and VCA domains of N-WASP. To exclude the possibility that unexpected endogenous cellular proteins influence their interaction, we examined the interaction of B-GBD and VCA domains using purified recombinant proteins in vitro. The GST-fused B-GBD (WT, T259E or T259A) fragments were purified from bacteria and subjected to in vitro binding test with bacterially purified His-tagged VCA fragment. As shown in Fig. 4E, T259E substitution only caused an increase in the binding of GBD fragment to VCA, which confirms the immunoprecipitation data of Fig. 4C,D.

An increase in the intramolecular interaction within the N-WASP protein would shift its structure from the hypothetical ‘open’ state, which exposes the VCA domain to Arp2/3, into the ‘closed’ state, which would inhibit the activation of Arp2/3. The VCA domain (amino acids 392–501) was shown to be capable of initiating actin polymerization in vitro with Arp2/3 complex in the pyrene-labeled actin polymerization assay (Prehoda et al., 2000). This VCA–Arp2/3-mediated actin polymerization is also repressed by the addition of B-GBD fragment (amino acids 178–274) (Prehoda et al., 2000). Using this assay, we examined the effect of Thr259 phosphorylation on the actin-polymerizing activity of N-WASP. As shown in Fig. 4F, the VCA fragment (red) greatly promoted actin polymerization, whereas addition of wild-type B-GBD (yellow) considerably inhibited the VCA-mediated actin polymerization. These data validated our assay system to test the auto-inhibition model of N-WASP to promote actin polymerization. Moreover, addition of B-GBD fragment containing a phospho-mimetic T259E mutation (green) led to a much larger inhibition of actin polymerization, compared with WT (yellow) or phospho-deficient T259A B-GBD (blue) fragments (Fig. 4F). In contrast to T259E substitution, addition of B-GBD fragment with T196E (blue) or T202E (purple) mutation failed to remarkably disrupt the VCA–Arp2/3-mediated actin polymerization and displayed a similar potency for the inhibition to WT B-GBD fragment (yellow) (Fig. 4G). These data suggest that Thr259 phosphorylation enhances the auto-inhibition of N-WASP and represses its actin-polymerizing activity. In addition, Thr259 phosphorylation appears to be enough to induce N-WASP protein to enter a ‘closed’ state by enhancing its intramolecular interaction. Interestingly, the double glutamate substitutions at T196 and T202 (2TE; blue) resulted in an inhibition of actin polymerization similarly to the level by the N-WASP T259E mutant (green), whereas the triple phospho-mimetic

mutation (3TE; purple) caused the largest inhibition against VCA–Arp2/3-mediated actin polymerization (Fig. 4H). These data suggest that single phosphorylation at Thr196 or Thr202 is not be sufficient to promote the intramolecular interaction of N-WASP, but double phosphorylation enables N-WASP to trigger its auto-inhibitory intramolecular interaction and repress actin polymerization. Moreover, double phosphorylation could enable completion and maintenance of N-WASP auto-inhibition.

Overall, these data demonstrate that Dyrk1A-mediated phosphorylation of the GBD of N-WASP tightly regulates the intramolecular interaction of N-WASP and subsequent Arp2/3-mediated actin polymerization.

Dyrk1A-mediated N-WASP phosphorylation inhibits filopodia formation in COS-7 cells

Proper actin polymerization through N-WASP–Arp2/3 signaling is important for diverse cellular processes, such as cell migration, morphogenesis, endocytosis, vesicle trafficking and phagocytosis (Mattila and Lappalainen, 2008). Actin filaments can assemble into many different structures within a cell, including filopodia and lamellipodia in migrating cells and dendritic spines of neurons (Goley and Welch, 2006). Filopodia are thin, finger-like protrusions composed of filamentous actin bundles (Mattila and Lappalainen, 2008). Before testing the effect of Dyrk1A-mediated phosphorylation of N-WASP on filopodia formation, we examined whether Dyrk1A colocalizes with N-WASP at actin filaments. After COS-7 cells were co-transfected with plasmids encoding V5-tagged Dyrk1A and EGFP-fused N-WASP, actin filaments were visualized using phalloidin–TRITC, which stains filamentous actin. As shown in Fig. 5A, immunostaining and fluorescence visualization of the three proteins revealed that they are colocalized in the cytoplasmic region. This finding was further supported by immunostaining of Dyrk1A–V5 and fluorescence visualization of EGFP–N-WASP and mCherry–LifeAct which probes endogenous actin filaments in a non-cytotoxic manner (Fig. 5B). We then examined the effect of GBD phosphorylation on the colocalization of N-WASP and actin filaments. COS-7 cells were co-transfected with plasmids encoding EGFP-fused N-WASP (WT, 3TE or 3TA) proteins and mCherry–LifeAct. As shown in Fig. 5C, EGFP–N-WASP was expressed in the nuclear and cytoplasmic regions regardless of phospho-mimetic 3TE or phospho-deficient 3TA mutation. Both 3TE and 3TA N-WASP mutants were also expressed in the regions close to plasma membrane and colocalized with actin filaments in a similar manner to that seen with WT N-WASP. Interestingly, overexpression of WT and 3TA N-WASP proteins caused filopodia-like protrusions, but they were not found with 3TE N-WASP. In addition, WT and 3TA N-WASP proteins, but not 3TE mutant, were simultaneously colocalized with actin filaments in the protrusions, suggesting a negative role for Dyrk1A-mediated phosphorylation of N-WASP in filopodia formation.

To further evaluate the effect of Dyrk1A-mediated N-WASP phosphorylation on filopodia formation, COS-7 cells were transfected with one of the EGFP-fused WT N-WASP constructs, its phospho-mimetic (3TE) or phospho-deficient (3TA) mutant at Thr196, Thr202 and Thr259 either alone or together with V5-tagged Dyrk1A. Analysis of actin filaments with phalloidin staining or mCherry–LifeAct expression revealed that the concomitant overexpression of WT N-WASP and Dyrk1A significantly inhibited filopodia formation, compared with that in cells transfected with N-WASP alone (50.5% for N-WASP WT vs 16.3% for N-WASP WT + Dyrk1A; $P<0.01$). However, the overexpression of Dyrk1A had no effect when WT N-WASP was not overexpressed (Fig. 5D,E). These data indicate that Dyrk1A-mediated N-WASP signaling is suppressed in a resting state. In addition, overexpression of the N-WASP 3TE mutant significantly decreased filopodia formation, compared with that in cells overexpressing WT N-WASP (50.5% for WT vs 23.5% for 3TE; $P<0.05$). These data suggest that the Dyrk1A-dependent phosphorylation of the GBD inhibit the filopodia-promoting activity of N-WASP (Fig. 5D,E). Although Dyrk1A overexpression did not significantly affect the reduced filopodia formation induced by expression of N-WASP 3TE, expression of the phospho-deficient N-WASP 3TA mutant significantly increased the formation of protruding filopodia structures (50.5% for WT vs 73.2% for 3TA; $P<0.05$). In addition, this effect was not considerably affected by concomitant overexpression of Dyrk1A. These results were consistent with the Dyrk1A-mediated phosphorylation effects on the binding affinity of N-WASP for Arp2/3 and further actin polymerization. In addition, these data further confirmed the hypothesis that the specific Dyrk1A phosphorylation of the GBD inhibits N-WASP activity, and dephosphorylation of the three Thr target residues might activate downstream signaling, ultimately leading to actin cytoskeleton and filopodia formation.

Knockdown of endogenous Dyrk1A promotes filopodia formation in COS-7 cells in an N-WASP-phosphorylation-dependent manner

We next examined the effect of reducing Dyrk1A expression on filopodia formation mediated by N-WASP phosphorylation. Plasmids encoding either EGFP labelled N-WASP 3TE or 3TA mutants were co-transfected into COS-7 cells with a construct encoding a short-hairpin RNA targeted against *Dyrk1A* mRNA (pSHAG-1-Dyrk1A-1) (Sitz et al., 2004). Analysis of the formation of actin structures by phalloidin staining or mCherry-LifeAct expression indicated that a reduction in Dyrk1A expression significantly enhanced filopodia formation in the presence of the EGFP control (15.0% for mock vs 53.8% for shDyrk1A-1; $P<0.001$; Fig. 6A,B). This result implies that the suppression of N-WASP-mediated downstream signaling induced by endogenous Dyrk1A is rescued by the depletion of Dyrk1A. Also, Dyrk1A knockdown significantly enhanced filopodia formation when WT N-WASP was concomitantly overexpressed (53.1% for N-WASP vs 76.3% for N-WASP + shDyrk1A-1; $P<0.05$; Fig. 6A,B). Furthermore, overexpression of the N-WASP 3TE mutant significantly decreased filopodia formation (53.1% for WT vs 27.1% for 3TE; $P<0.01$), irrespective of Dyrk1A expression, whereas the N-WASP-3TA mutant significantly increased filopodia formation up to the level produced by the combinatory effects of WT N-WASP and Dyrk1A knockdown (53.1% for WT vs 78.5% for 3TA; $P<0.01$; Fig. 6A,B). The stimulatory effect of Dyrk1A knockdown on COS-7 cell filopodia formation was confirmed with another shDyrk1A construct that targets to a different region of *Dyrk1A* mRNA (pSHAG-1-Dyrk1A-2) (Sitz et al., 2004), indicating that the results did not come from the off-target side effects of knockdown experiments (Fig. 6A,C). These data confirm that Dyrk1A-mediated phosphorylation inhibits N-WASP activity required for actin cytoskeleton and subsequent filopodia formation.

Dyrk1A-induced phosphorylation of the GBD inhibits N-WASP activity and promotes dendritic spine formation

To validate the inhibitory effects of N-WASP GBD phosphorylation with another actin filament assembly model, we examined dendritic spine formation in primary hippocampal neurons in the absence or presence of WT N-WASP or N-WASP 3TE mutant. Dendritic spines are small protrusions originating from dendritic shafts of neurons and their cytoskeletons are mainly composed of actin filaments inserted into postsynaptic density, which tend to exclude microtubules and intermediate

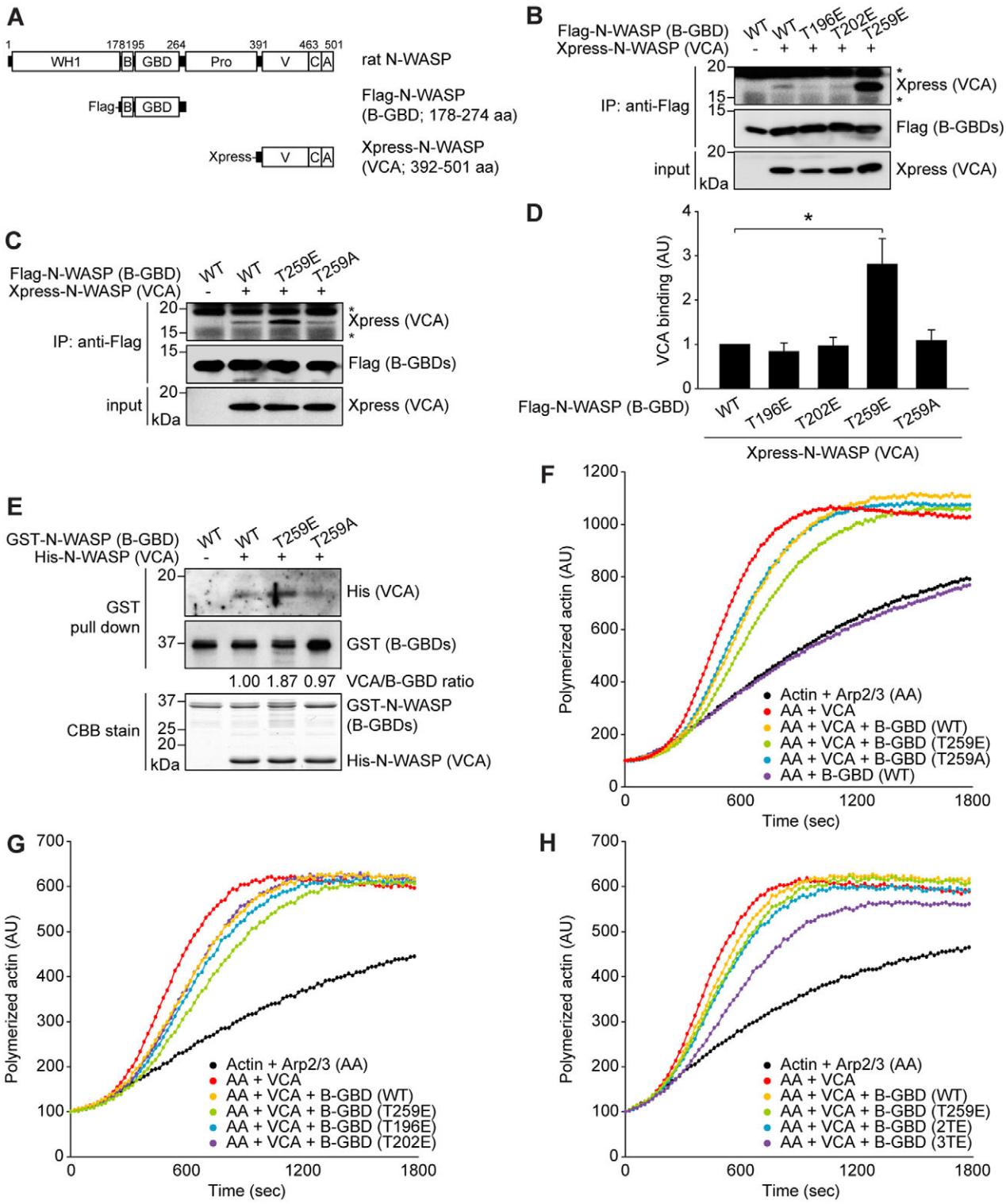

Fig. 4. See next page for legend.

filaments (Kaech et al., 2001). After rat embryonic hippocampal neurons were transfected with plasmids encoding EGFP-fused WT N-WASP or a phospho-mimetic 3TE mutant, actin filament formation was visualized using mCherry–LifeAct. As shown in Fig. 7A–D, the average density of spines was much higher in cells overexpressing WT N-WASP (0.77±0.11, $P<0.001$), compared with cells expressing EGFP (0.52±0.11; Fig. 7A–C). These results verify the positive role for N-WASP in dendritic spine formation, as previously reported (Wegner et al., 2008). By contrast, overexpression of the N-WASP 3TE mutant failed to increase the densities of neural spine formation, compared with levels in the EGFP control (0.52±0.08). In addition, the length of the dendritic spines was increased in the presence of overexpression of WT N-WASP, whereas the N-WASP 3TE mutant had no effect, compared to the EGFP control.

Finally, we examined whether the inhibitory action of Dyrk1A overexpression or the stimulatory effect of N-WASP 3TA mutant also applies to the dendritic spine formation in hippocampal neurons. The primarily cultured hippocampal neurons were transfected with EGFP-fused WT N-WASP or N-WASP 3TA mutant either alone or with V5-tagged Dyrk1A. As shown in Fig. 7E,F, Dyrk1A overexpression caused a significant decrease in dendritic spine number (0.27±0.05, $P<0.001$), which was promoted by overexpression of WT N-WASP (0.47±0.06), similarly to the mock transfection levels (0.34±0.09). However, the phospho-deficient 3TA mutation of N-WASP led to a significant increase in dendritic spine formation (0.55±0.09, $P<0.001$) even upon overexpression of Dyrk1A (Fig. 7F).

These data suggest that Dyrk1A-mediated GBD phosphorylation negatively regulates the dendritic spine formation of CNS neurons by inhibiting N-WASP activity.

Fig. 4. Dyrk1A-induced phosphorylation of the GBD promotes the intramolecular interaction of N-WASP and inhibits its downstream binding to Arp2/3 and consequent actin polymerization. (**A**) Schematic representation of N-WASP fragments (FLAG-tagged B-GBD and Xpress-tagged VCA) used to test the intramolecular interaction of N-WASP. (**B**) Co-immunoprecipitation and immunoblot analysis of the interaction between the Xpress-tagged N-WASP-VCA fragment and FLAG-tagged phospho-mimetic B-GBD mutant, which is substituted at a single residue. (**C**) Co-immunoprecipitation and immunoblot analysis of the interaction between Xpress-tagged N-WASP-VCA and either FLAG-tagged B-GBD T259E or T259A mutants. (**D**) The band intensity of bound VCA fragments was measured using Multi Gauge software (Fujifilm) and the data are expressed as mean ± s.e.m. ($n=3$; *$P<0.05$). (**E**) In vitro binding test between recombinant GST-fused B-GBD and His-tagged VCA fragments. The purified B-GBD and VCA proteins were incubated with glutathione–Sepharose beads at 4℃ overnight, and the protein complexes were pulled down and subjected to immunoblotting analysis with anti-His antibody. The lower panel indicates Coomassie Brilliant Blue (CBB) staining of each protein input. The intensity of bound VCA fragments was measured, and the ratio of bound VCA levels to the precipitated B-GBD levels is presented as arbitrary data. (**F**) In vitro pyrene-labeled actin polymerization assay with GST–VCA (1.0 μg) and GST–B-GBD fragments (0.5 μg) having phospho-mimetic (T259E) or phospho-deficient (T259A) substitution at Thr259. The reaction with only actin and Arp2/3 complex (AA; black) served as the baseline of actin polymerization. (**G**,**H**) In vitro pyrene-labeled actin polymerization assay with GST-B-GBD fragments having phospho-mimetic single (G), double or triple (H) substitution at Thr196, Thr202 and/or Thr259 residues. The 2TE mutant indicates N-WASP having double glutamate substitution at both T196 and T202 residues and the 3TE indicates triple glutamate mutation at all three residues.

Discussion

Dyrk1A is a proline-directed serine/threonine kinase that is involved in various cellular processes including gene transcription, endocytosis, cell proliferation, and cell death; it mediate these effects by the phosphorylation of more than 20 substrates (Park et al., 2009a; Park et al., 2009b). Some recent studies implicate Dyrk1A in regulating the function of microtubule-associated proteins and neurite formation. For example, stable overexpression of Dyrk1A increases levels of the phosphorylated microtubule-associated protein tau and its intracellular inclusions in rat embryonic hippocampal progenitor H19-7 cells. This inhibits the cells from differentiating into neurons (Park et al., 2007). In addition, specific knockdown of Dyrk1A reduces the neurite length of embryonic cortical neurons and increases neurite branching (Scales et al., 2009). Treatment of hippocampal neurons with harmine, a specific inhibitor for Dyrk1A, also significantly reduces the neurite number (Gockler et al., 2009). The compromised neuritogenesis is thought to result from a decrease in the level of Dyrk1A-mediated phosphorylation of microtubule-associated phosphoprotein MAP1B (Scales et al., 2009). In spite of this putative correlation between Dyrk1A and microtubule-associated proteins, the role of Dyrk1A in actin filament assembly and dynamics has not been fully characterized. Here, we provide evidence on the negative regulatory function of Dyrk1A on N-WASP activity and actin polymerization.

The present study demonstrates that Dyrk1A interacts with and directly phosphorylates N-WASP. The Dyrk1A-mediated multiple phosphorylation within the GBD (Thr196, Thr202 and Thr259) strengthened the intramolecular interaction of N-WASP without affecting its ability to bind to the upstream GTPase Cdc42. The GBD phosphorylation results in an auto-inhibition of N-WASP activity and a consequent reduction of Arp2/3-mediated actin filament assembly. Correspondingly, analyses of filopodia formation in COS-7 cells and dendritic spine formation in rat hippocampal neurons demonstrate that the phosphorylation-mimic 3TE mutant of N-WASP has much lower activity than WT N-WASP in regards to stimulation of actin polymerization, and this can be reversed by the phospho-deficient 3TA mutant.

The intramolecular interaction of N-WASP is a primary regulator of N-WASP activity. Accordingly, the VCA domain of N-WASP can activate downstream Arp2/3, whereas its action is auto-inhibited by its interaction with the GBD region (Kim et al., 2000; Prehoda et al., 2000). Data from co-immunoprecipitation and in vitro binding experiments using N-WASP VCA and B-GBD fragments, and testing the effect of its phospho-mimetic glutamate substitution mutant reveal that the Thr259 residue is the most effective targeting site of Dyrk1A. This site specifically regulates the intramolecular interaction of N-WASP (Fig. 4B–E). The importance of Thr259 phosphorylation is further supported by in vitro actin polymerization assay (Fig. 4F,G) and by the occurrence of Dyrk1A-mediated Thr259 phosphorylation in HEK293 cells (supplementary material Fig. S2). Interestingly, based on the finding that the Thr259 residue and neighboring amino acid sequences of N-WASP are completely conserved in human, rat and mouse genes, we speculate that the segment around the Thr259 residue might have an important role in regulating N-WASP function (Fig. 8A). Moreover, comparison of the amino acid sequences between N-WASP and WASP/WAVE family proteins reveals that the Thr259 of N-WASP corresponds to the Ser310 residue of WAVE1 (Fig. 8B). Intriguingly, the Ser310 residue of WAVE1 is phosphorylated

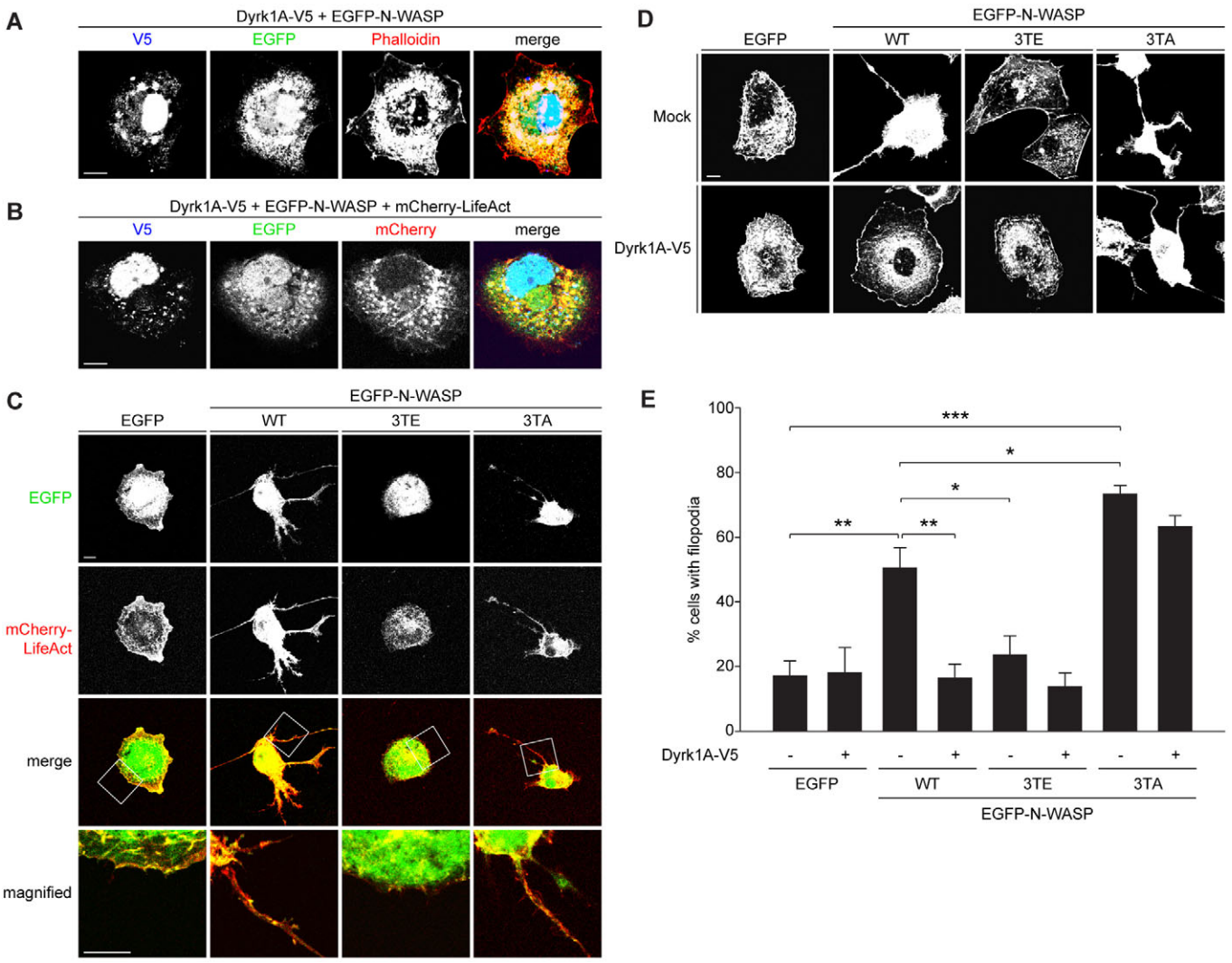

Fig. 5. Dyrk1A overexpression inhibits filopodia formation in COS-7 cells through N-WASP phosphorylations of GBD. (**A**,**B**) Representative confocal images for the colocalization of V5-tagged Dyrk1A (blue), EGFP-fused N-WASP (green), and actin filaments (red) stained by phalloidin–TRITC (A) or mCherry–LifeAct (B) in COS-7 cells are shown. (**C**) Representative confocal images for the colocalization of either EGFP-fused WT N-WASP, phospho-mimetic (3TE) or phospho-deficient (3TA) mutants (green), and actin probed with mCherry–LifeAct (red) in COS-7 cells are shown. (**D**) Representative confocal images of actin filaments in COS-7 cells (by phalloidin-TRITC) are presented. (**E**) Effect of Dyrk1A overexpression and N-WASP phosphorylations on filopodia formation in COS-7 cells. Cells with a minimum of three filopodia measuring at least 10 μm in length were visualized by mCherry–LifeAct and scored as being 'with filopodia'. Data are expressed as mean ± s.e.m. ($n=5$; *$P<0.05$, **$P<0.01$ and ***$P<0.001$). Scale bars: 10 μm.

by cyclin-dependent kinase 5 (Cdk5), which subsequently inhibits the actin-polymerizing activity of WAVE1 (Kim et al., 2006). Therefore, it could be hypothesized that N-WASP and WAVE1 share a similar regulatory mode of actin polymerization activity through phosphorylation; for example, Dyrk1A for N-WASP and Cdk5 for WAVE1. However, WAVE family proteins lack the inhibitory GBD and constitutively form a hetero-pentameric complex with Sra1, Nap1, Abi and HSPC300 (Takenawa and Suetsugu, 2007). Recent structural analysis of WAVE regulatory complex revealed that WAVE1 VCA domain binds to a conserved surface of Sra1 and a part of WAVE1 with a meandering region (Chen et al., 2010). Therefore, the regulatory mechanism of WAVE proteins might be different from that of N-WASP and WASP proteins.

The phospho-mimetic mutations of N-WASP at Thr196 and Thr202 had no considerable effect on its intramolecular interaction (Fig. 4B,D) and Arp2/3-mediated actin polymerization (Fig. 4G), even though they were considerably phosphorylated by Dyrk1A (Fig. 2D,E). However, in vitro actin polymerization assay provides insight on the role of Thr196 and Thr202 phosphorylation. Although there was no remarkable inhibition by single T196E or T202E mutation (Fig. 4G), their double glutamate substitutions at T196 and T202 (2TE) inhibited actin polymerization to a similar level as the N-WASP T259E mutant (Fig. 4H). These data suggest that single phosphorylation at Thr196 or Thr202 residue might not be sufficient to promote the intramolecular interaction of N-WASP, but their double phosphorylation could trigger the binding of the B-GBD fragment to the VCA domain. That is, the intramolecular interaction of N-WASP can be strengthened by Dyrk1A through either single phosphorylation at Thr259 or double phosphorylation at Thr196 and Thr202. In addition, the triple

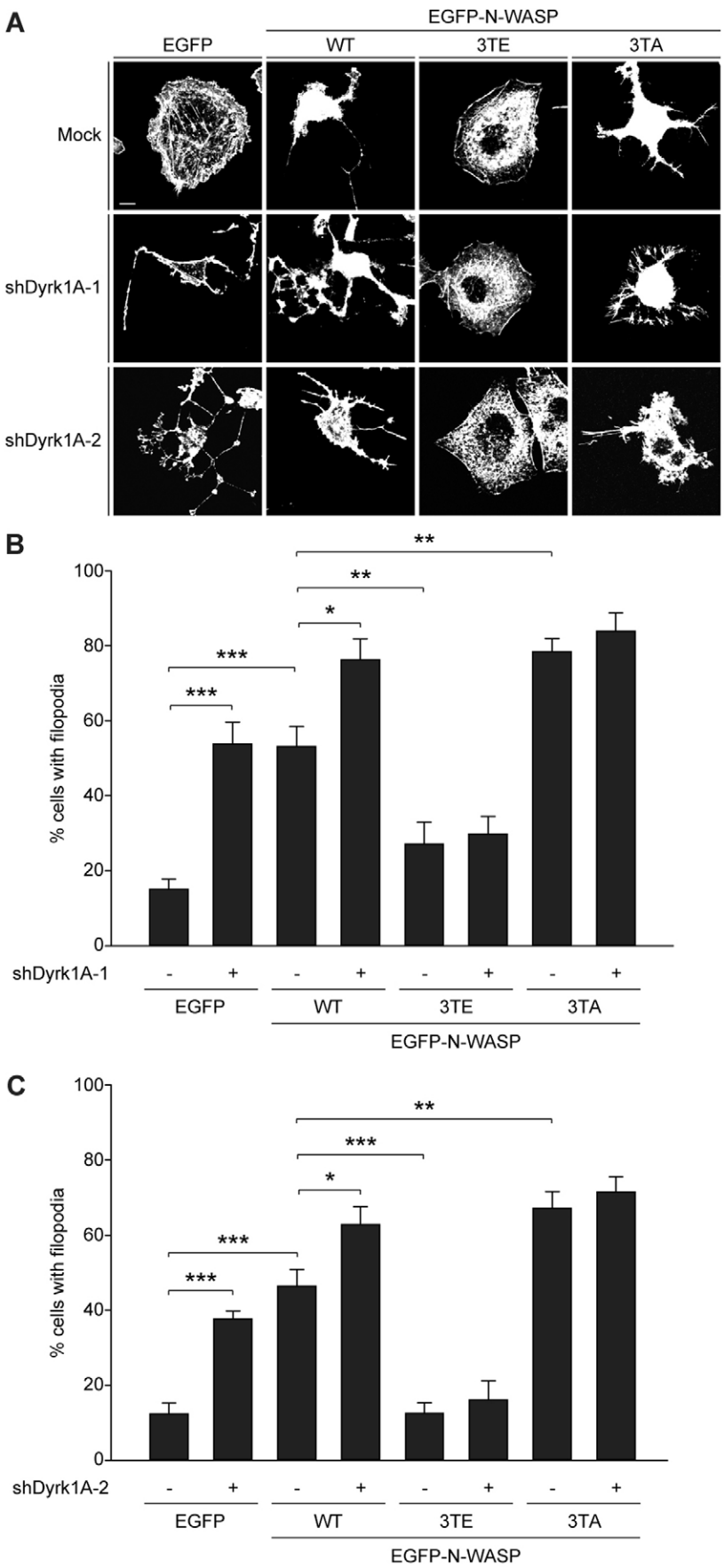

Fig. 6. Knockdown of Dyrk1A expression promotes filopodia formation in COS-7 cells through reduced phosphorylation of N-WASP-GBD. (**A**) Representative confocal images of actin filaments stained by phalloidin-TRITC are shown in COS-7 cells. Scale bar: 10 µm. (**B**,**C**) Effect of Dyrk1A knockdown and N-WASP phosphorylation on filopodia formation in COS-7 cells. Cells with a minimum of three filopodia measuring at least 10 µm in length were visualized by mCherry–LifeAct or phalloidin-TRITC) and scored as being 'with filopodia'. Data are expressed as mean ± s.e.m. ($n=6$; *$P<0.05$, **$P<0.01$ and ***$P<0.001$).

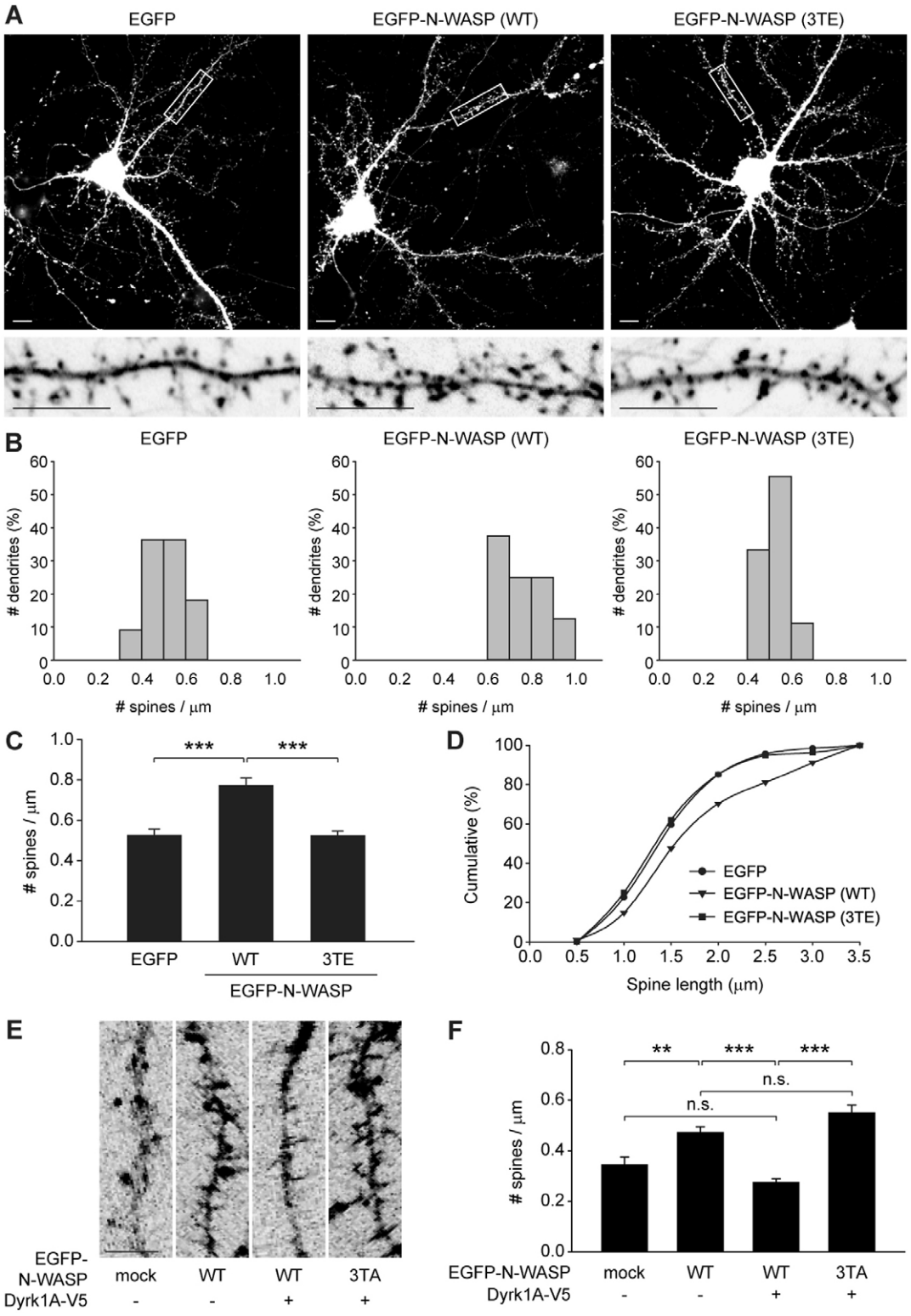

Fig. 7. Phosphorylation mimic with triple mutations at the three targeting residues within the GBD inhibits N-WASP activity to promote dendritic spine formation. (**A**) Representative images of rat hippocampal neurons transfected with either WT N-WASP or an N-WASP 3TE mutant. High-magnification views are of the regions enclosed in rectangles. Images are inverted for clarity. (**B**,**C**) Changes in the number of dendritic spines by the phospho-mimetic substitution within the GBD of N-WASP. Histograms of the number of dendritic spines per micrometer in the transfected neurons (B) and comparison of the average numbers of spines (C) are presented. Data are expressed as mean ± s.e.m. (n=4; ***P<0.001). (**D**) Cumulative frequency and distribution of dendritic spine lengths in the transfected neurons. (**E**,**F**) Effect of Dyrk1A and the phospho-deficient N-WASP 3TA mutant on the dendritic spine numbers in cultured hippocampal neurons. Representative images of dendritic spines transfected as indicated (E) and the comparison of average spine numbers (F) are presented. Images are inverted for clarity. Data are expressed as mean ± s.e.m. (n=4; **P<0.01 and ***P<0.001). Scale bars: 10 μm.

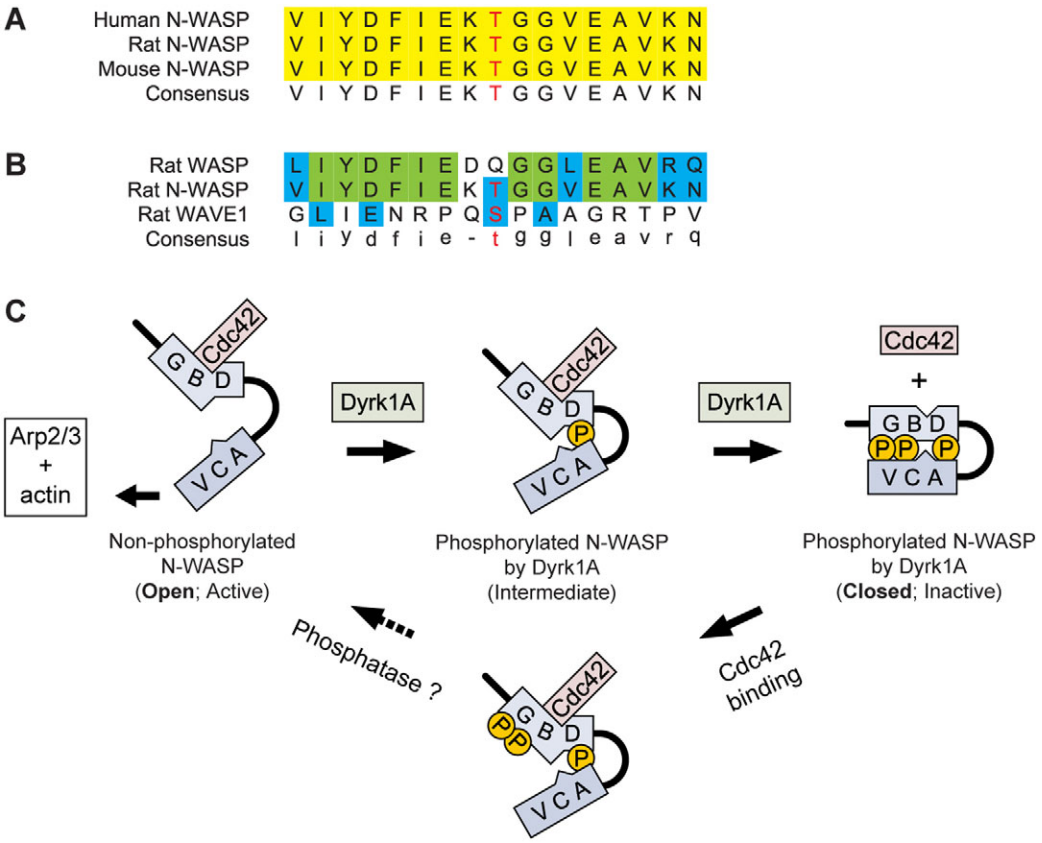

Fig. 8. A model for the regulation of intramolecular N-WASP interaction by Dyrk1A-induced phosphorylation of the GBD. (**A**) Sequence comparison of human, rat and mouse N-WASP proteins around the Dyrk1A-targeting Thr259 residue. Thr259 is marked in red, and completely conserved residues are labeled with yellow. (**B**) Sequence comparison and conservation of N-WASP Thr259 and WAVE1 Ser310 residues are marked in red. The identical residues are labeled with green, and similar residues are indicated with blue. (**C**) A model depicting the regulatory modes of intramolecular N-WASP interaction through Dyrk1A-induced phosphorylation. There are two different functional states of N-WASP protein depending on its structure; the 'open' state for active N-WASP activity, which forms when it is not phosphorylated, and the 'closed' inhibitory state, which forms in response to Dyrk1A-mediated phosphorylation within the GBD.

phospho-mimetic mutant of N-WASP (3TE) inhibited actin polymerization much more than the T259E or 2TE mutant did (Fig. 4H). Based on these findings, our working hypothesis is that single phosphorylation at Thr259 might be enough to promote the intramolecular interaction of N-WASP. In addition, it would be a more effective way than double phosphorylation at Thr196 and Thr202 to achieve N-WASP transition into the inhibitory (closed) state (Fig. 8C). Furthermore, double phosphorylation of N-WASP at T196 and T202 appears to contribute additionally to the completion and maintenance of the auto-inhibitory action of N-WASP-Thr259 phosphorylation (Fig. 8C). The Dyrk1A-mediated threonine phosphorylation of N-WASP at residues 196, 202 and 259 might eventually drive N-WASP to an auto-inhibitory state by enhancing the intramolecular interaction, as shown in an in vitro pyrene–actin assay with full-length WT N-WASP and its triple point mutant protein with glutamate substitution (supplementary material Fig. S3). By contrast, these three Thr residues of N-WASP should be dephosphorylated for its transition into the active (open) state, which leads to the activation of downstream signaling pathway and actin filament assembly. These results should be confirmed by further studies to identify the specific phosphatase(s) that is involved in the dephosphorylation of the GBD of N-WASP.

There have been several studies thus far demonstrating the phosphorylation of N-WASP and its functional alteration for actin polymerization. For example, Src family kinase phosphorylates a tyrosine residue (Tyr253) within the GBD, which stimulates N-WASP activity to promote neurite extension (Suetsugu et al., 2002). The phosphorylation of N-WASP at Thr residues also affects the protein stability, leading to degradation by the proteasome (Suetsugu et al., 2002). Several groups have identified Ser and Tyr phosphorylation within the GBD or VCA domain of the WASP protein, but the in vivo functions of these phosphorylation events were not characterized (Dovas and Cox, 2010). Here, we present a novel regulatory mechanism for N-WASP activity through Dyrk1A phosphorylation and modulation of its intramolecular interaction.

These data might contribute to the understanding of not only the regulation of intracellular actin polymerisation, but also the neuropathological features observed in DS patients. The *DYRK1A* gene is located within the Down syndrome critical region (DSCR) on human chromosome 21, which is assumed to mediate many neurological symptoms associated with DS (Park et al., 2009a; Park et al., 2009b). In addition, *Dyrk1A* transgenic mice exhibit a significant alteration in hippocampal-dependent memory tasks and synaptic plasticity, which are typical clinical

manifestations of both DS and Alzheimer's disease (Ahn et al., 2006; Ryoo et al., 2007; Ryoo et al., 2008). With respect to DS and the proposed multiple roles for Dyrk1A in the neuronal system, the present finding that Dyrk1A is also involved in the regulation of dendritic spine formation through N-WASP phosphorylation is important. The loss, change in size, and/or morphological disruption of dendritic spines have been suggested to contribute to learning and memory deficits, which are observed in many neurological diseases, including DS (Calabrese et al., 2006; Kasai et al., 2003). Moreover, most DS patients suffer from mental retardation with cognitive abnormalities and deficits in learning and memory (Park et al., 2009a; Park et al., 2009b). They also exhibit arrested synaptogenesis and a significant reduction in the number of hippocampal dendritic spines (Ferrer and Gullotta, 1990; Wisniewski et al., 1984). In this context, the present findings could provide a possible link between Dyrk1A and the altered synaptogenesis and spinogenesis observed in DS patients. Furthermore, the present finding could contribute to expanding our current understanding on diverse actin-based cellular processes such as cell migration, morphogenesis, endocytosis, vesicle trafficking, phagocytosis and neuronal differentiation.

Materials and Methods

Materials

Two different anti-Dyrk1A antibodies were purchased from Abnova Corporation (Taipei City, Taiwan) and Cell Signaling Technology (Beverly, MA). Rabbit polyclonal anti-N-WASP and anti-Arp2 antibodies were purchased from Cell Signaling Technology. The following reagents were purchased from Invitrogen (Carlsbad, CA); anti-Xpress, anti-V5, Alexa-Fluor-405-conjugated anti-mouse IgG, Alexa-Fluor-546-conjugated anti-rabbit IgG, horseradish-peroxidase-conjugated IgG (anti-mouse and anti-rabbit IgG), Dulbecco's modified Eagle's medium (DMEM), Hank's balanced salt solution (HBSS), B-27 supplement, Opti-MEM I, Ni^{2+}-NTA agarose beads and BL21 cells. Anti-FLAG antibody and agarose beads were purchased from Sigma (St Louis, MO). Anti-GST antibody and normal rabbit IgG were purchased from Santa Cruz Biotechnology (Santa Cruz, CA). Enhanced chemiluminescence reagent and [γ-^{32}P]ATP were purchased from PerkinElmer Life and Analytical Sciences (Waltham, MA). All other reagents were purchased from Sigma and USB Corporation (Cleveland, OH).

DNA constructs and RNA interference

Mammalian constructs encoding 6×His-Xpress-tagged rat Dyrk1A [wild type (WT) and K188R], V5–6×His-tagged Dyrk1A (WT) and bacterial constructs encoding 6×His-tagged Dyrk1A (WT and K188R) were generated as previously described (Park et al., 2007; Park et al., 2010).

To generate a construct encoding FLAG-tagged N-WASP, the rat N-WASP gene (*Wasl*) was amplified using PCR. The PCR product was then subcloned into a pRK5-FLAG vector between *Mlu*I and *Not*I sites. To assess the intramolecular binding between the basic plus GTPase-binding domain (B-GBD; amino acids 178–274) and the VCA domain (amino acids 392–501) within the N-WASP protein, plasmids encoding FLAG-tagged N-WASP B-GBD and Xpress-tagged N-WASP VCA were generated using PCR amplification of the rat N-WASP gene. Each PCR product was then subcloned into either pRK5-FLAG vector between the *Mlu*I and *Not*I sites or into the pcDNA4/HisMax vector between *Eco*RI and *Xho*I sites. To generate EGFP-fused N-WASP, the rat N-WASP gene was amplified using PCR. The PCR product was then subcloned into a pEGFP-C2 vector between *Xho*I and *Eco*RI sites. To purify the bacterial recombinant 6×His-tagged N-WASP proteins, the full-length rat N-WASP gene was amplified using PCR. The PCR product was then subcloned into a pET-28a(+) vector between *Eco*RI and *Xho*I sites. Truncated forms of rat *Wasl* were also subcloned into a pET-28a(+) vector. Detailed information of the primers used is in supplementary material Table S1.

The QuikChange XL site-directed mutagenesis kit (Stratagene; La Jolla, CA) was used for the site-directed mutagenesis according to the manufacturer's protocol. The pET-28a(+)-N-WASP, pRK5-FLAG-N-WASP, and pEGFP-C2-N-WASP constructs were amplified using PCR. The primer sequences for the mutagenesis are listed in supplementary material Table S2. The double or triple substitution was carried out by two rounds of mutagenesis PCR with combinations of the primers in the list.

In addition, we obtained a mammalian construct encoding glutathione S-transferase (GST)-fused Cdc42-V12 (pEBG-Cdc42-V12) from Kang-Yell Choi (Yonsei University, Seoul, Korea). Two plasmids for the specific knockdown of endogenous Dyrk1A [pSHAG-1-Dyrk1A-1 (J162.1) and pSHAG-1-Dyrk1A-2 (J163)] was generously provided by Beat Lutz (Max Planck Institute of Psychiatry, Munich, Germany) (Sitz et al., 2004).

Cell culture, DNA transfection and primary rat hippocampal neurons

HEK293 and COS-7 cells were cultured at 37℃ in DMEM containing 10% heat-inactivated FBS (Invitrogen), 100 U/ml penicillin and 100 μg/ml streptomycin (Invitrogen). DNA transfections were performed using Lipofectamine plus reagents (Invitrogen), according to the manufacturer's protocol.

All animal experiments were performed in accordance with the guidelines set forth by the Yonsei Laboratory Animal Research Center for the proper care and use of laboratory animals. Cultured hippocampal neurons were prepared from E18 fetal Sprague-Dawley rats as previously described (Lee et al., 2006). The hippocampal neurons were dissected and plated on coverslips coated with poly-D-lysine. They were grown in Neurobasal medium (Invitrogen) supplemented with 2% B-27 and 0.5 mM L-glutamine. After 10 days in vitro (DIV) culture, transient transfections of hippocampal neurons were performed using the calcium phosphate precipitation method (Lee et al., 2006). Cells were incubated for 60–90 minutes with the transfection mixture before washing and fresh growth medium was added.

Immunoprecipitation and immunoblot analyses

Preparation of cell lysates, immunoprecipitation and immunoblot analyses were performed as previously described (Park et al., 2010).

Purification of recombinant proteins

Bacterial expression of recombinant N-WASP and Dyrk1A proteins in BL21 cells and their purifications were performed as previously described (Park et al., 2010). Bacterial recombinant protein expression was induced with 0.1 mM isopropyl β-D-1-thiogalactopyranoside for 2 hours at 30℃ (with shaking at 200 r.p.m.), pelleted by centrifugation at 3000 ***g*** for 15 minutes at 4℃ and the cells were sonicated in either lysis buffer (50 mM NaH_2PO_4, pH 8.0, 300 mM NaCl, 15 mM imidazole and 2 mM phenylmethylsulfonyl fluoride) for His-tagged proteins or PBS (pH 7.4) for GST-fused proteins. After clearing by centrifugation at 3000 ***g*** for 15 minutes at 4℃, the supernatant was incubated with Ni^{2+}-NTA agarose beads for His-tagged proteins or glutathione-Sepharose beads for GST-tagged proteins overnight at 4℃. The beads were then washed five times with either washing buffer (50 mM NaH_2PO_4, pH 8.0, 300 mM NaCl, 100–250 mM imidazole, and 2 mM phenylmethylsulfonyl fluoride) for His-tagged proteins or PBS for GST-fused proteins, and the recombinant proteins were eluted by adding either elution buffer (50 mM NaH_2PO_4, pH 8.0, 300 mM NaCl, 250–500 mM imidazole and 2 mM phenylmethylsulfonyl fluoride) for His-tagged proteins or 10 mM reduced glutathione buffer for GST-fused proteins.

In vitro kinase assay

Preparation of anti-Dyrk1A immunocomplexes or bacterial recombinant Dyrk1A protein and the in vitro kinase assays were performed as previously described (Park et al., 2010). HEK293 cells were transfected with the plasmid encoding Xpress-tagged WT or K188R Dyrk1A for 24 hours. Cells were then lysed in 1% Nonidet P40 lysis buffer and lysates were immunoprecipitated with anti-Xpress antibody overnight at 4℃. The immunocomplexes were then incubated with 30 μl of a 1:1 suspension of Protein-A–Sepharose beads for 2 hours at 4℃ and centrifuged at 13,000 ***g*** for 30 seconds at 4℃. The samples were washed twice with 1% Nonidet P40 lysis buffer, and twice with 1× Dyrk1A buffer (20 mM HEPES, pH 7.4, 20 mM $MgCl_2$, 5 mM $MnCl_2$ and 1 mM dithiothreitol). For the in vitro kinase reaction, either anti-Dyrk1A immunocomplexes or purified recombinant Dyrk1A proteins were mixed with 1 μg of recombinant N-WASP as a substrate in 1× Dyrk1A buffer containing 0.2 mM sodium orthovanadate and 10 μM ATP. The reaction was initiated by adding 10 μCi [γ-^{32}P]ATP and allowed to proceed for 15 minutes at 30℃. After stopping the reaction by adding 5× SDS-PAGE sample buffer and boiling for 5 minutes, the protein samples were resolved by SDS-PAGE and the incorporated [γ-^{32}P] radioisotope was detected by autoradiography.

In vitro binding assay

Purified recombinant Dyrk1A proteins were incubated with recombinant N-WASP protein and anti-Dyrk1A antibody overnight at 4℃. The mixture was then incubated with 30 μl of a 1:1 suspension of Protein-A–Sepharose beads for 2 hours at 4℃ with gentle rotation, followed by immunoprecipitation and immunoblot analyses. To examine the binding between N-WASP and Cdc42 in vitro, ectopically expressed GST–Cdc42 (V12) or GST proteins in HEK293 cell lysates (1 mg) were precipitated with glutathione-Sepharose beads, washed three times with lysis buffer, and incubated with 2.5 μg of bacterially purified N-WASP (WT or 3TE) proteins overnight at 4℃. The proteins were then precipitated, washed three times with lysis buffer, and analyzed by SDS-PAGE and immunoblotting. In addition, the in vitro binding between GST–B-GBD and

His–VCA fragments was determined after incubation of each protein (2 μg) overnight at 4℃, precipitation next day and washing with lysis buffer three times.

In vitro actin polymerization assay

Actin polymerization was monitored by the increase in fluorescence of pyrene-labeled actin using the Actin Polymerization Biochem kit (Cytoskeleton), according to the manufacturer's protocol. Polymerization was initiated by adding Actin Polymerization Buffer stock (final concentration: 50 mM KCl, 2 mM $MgCl_2$, and 1 mM ATP) to mixtures of 5 mM Tris-HCl (pH 8.0), 0.2 mM $CaCl_2$, 0.2 mM ATP, pyrene-labeled actin (30 ng/ μl), Arp2/3 complex (13 nM; Cytoskeleton), GST–VCA (1.0 μg; Cytoskeleton) and 0.5 μg of the purified GST–B-GBD fragments. Fluorescence (excitation: 355±20 nm; emission: 405±5 nm) was measured at 25℃ using a VICTOR X3 multilabel plate reader (PerkinElmer).

Immunocytochemistry

COS-7 cells and primary neurons were washed twice with PBS and fixed with 4% paraformaldehyde and 4% sucrose in PBS for 15 minutes. If necessary, cells were permeabilized with 0.25% Triton X-100 in PBS for 5 minutes and washed twice with PBS. The samples were then blocked with 10% bovine serum albumin in PBS for 30 minutes. To visualize the V5-tagged Dyrk1A, cells were stained with mouse monoclonal anti-V5 antibody, and anti-mouse IgG Alexa Fluor 405 conjugate (or Alexa Fluor 546 conjugate) was used to detect the primary V5 antibody. To visualize the endogenous actin filaments, cells were stained with 0.1 μM phalloidin–TRITC (Sigma) in PBS (pH 7.4) for 15 minutes. Confocal microscopy images were obtained using a LSM 510 META confocal microscope (Carl Zeiss, Göttingen, Germany) and data were processed using the Zeiss LSM Image Browser (Carl Zeiss). The fluorescent microscopic images were obtained using an Olympus IX-71 inverted microscope (Olympus Optical; Tokyo, Japan) with a 40×, 1.0 NA oil lens using a CoolSNAP-Hq CCD camera (Princeton Instruments, Trenton, NJ), driven by MetaMorph imaging software (Universal Imaging Corporation, Downingtown, PA).

Production of polyclonal antisera against phosphorylated Thr259 N-WASP

Rabbit polyclonal N-WASP phospho-Thr259 antisera were generated by Ab Frontier (Seoul, Republic of Korea) using a phosphorylated peptide (IYDFIEKpTGGVEAVK) corresponding to amino acids 252–266 of rat N-WASP. Rabbit antisera were used for immunoblotting analysis at a dilution of 1:3000.

Data deposition

The sequences reported in this paper have been deposited in the GenBank database [Accession No. NP_036923 (rat Dyrk1A) and BAA21534 (rat N-WASP)].

Statistical analysis

Group means were compared using the Student's *t*-test. *P* values less than 0.05 were considered significant.

Acknowledgements

The authors are deeply grateful to Kang-Yell Choi and Beat Lutz for generously providing plasmids. We also thank J. Lee, Y. J. Oh, I. K. Chung, and S. H. Lee for their critical comments and helpful discussions.

Funding

This study was supported by a grant from the Korea Healthcare Technology R&D Project, Ministry for Health, Welfare & Family Affairs, Republic of Korea [grant number A092004] to K.C.C. and W.J.S. This work was also supported by the Brain Research Center of the 21st Century Frontier Research Program Technology [grant number 2009K-001251] to K.C.C., which is funded by the Ministry of Education, Science and Technology (MEST), Republic of Korea. This work was also partially supported by a National Research Foundation of Korea (NRF) grant funded by MEST [grant number 2010-0018916] to K.C.C., a Basic Science Research Program through NRF [grant number 2011-0001176] to K.C.C., and a grant from the Korea Science and Engineering Foundation [grant number R01-2007-000-11910-0] to W.J.S.

Supplementary material available online at
http://jcs.biologists.org/lookup/suppl/doi:10.1242/jcs.086124/-/DC1

References

Adayev, T., Chen-Hwang, M. C., Murakami, N., Wang, R. and Hwang, Y. W. (2006). MNB/DYRK1A phosphorylation regulates the interactions of synaptojanin 1 with endocytic accessory proteins. *Biochem. Biophys. Res. Commun.* **351**, 1060-1065.

Ahn, K. J., Jeong, H. K., Choi, H. S., Ryoo, S. R., Kim, Y. J., Goo, J. S., Choi, S. Y., Han, J. S., Ha, I. and Song, W. J. (2006). DYRK1A BAC transgenic mice show altered synaptic plasticity with learning and memory defects. *Neurobiol. Dis.* **22**, 463-472.

Aspenstrom, P., Lindberg, U. and Hall, A. (1996). Two GTPases, Cdc42 and Rac, bind directly to a protein implicated in the immunodeficiency disorder Wiskott-Aldrich syndrome. *Curr. Biol.* **6**, 70-75.

Calabrese, B., Wilson, M. S. and Halpain, S. (2006). Development and regulation of dendritic spine synapses. *Physiology* (*Bethesda*) **21**, 38-47.

Chen, Z., Borek, D., Padrick, S. B., Gomez, T. S., Metlagel, Z., Ismail, A. M., Umetani, J., Billadeau, D. D., Otwinowski, Z. and Rosen, M. K. (2010). Structure and control of the actin regulatory WAVE complex. *Nature* **468**, 533-538.

Chen-Hwang, M. C., Chen, H. R., Elzinga, M. and Hwang, Y. W. (2002). Dynamin is a minibrain kinase/dual specificity Yak1-related kinase 1A substrate. *J. Biol. Chem.* **277**, 17597-17604.

Dovas, A. and Cox, D. (2010). Regulation of WASp by phosphorylation: activation or other functions? *Commun. Integr. Biol.* **3**, 101-105.

Ferrer, I. and Gullotta, F. (1990). Down's syndrome and Alzheimer's disease: dendritic spine counts in the hippocampus. *Acta Neuropathol.* **79**, 680-685.

Gockler, N., Jofre, G., Papadopoulos, C., Soppa, U., Tejedor, F. J. and Becker, W. (2009). Harmine specifically inhibits protein kinase DYRK1A and interferes with neurite formation. *FEBS J.* **276**, 6324-6337.

Goley, E. D. and Welch, M. D. (2006). The ARP2/3 complex: an actin nucleator comes of age. *Nat. Rev. Mol. Cell Biol.* **7**, 713-726.

Himpel, S., Tegge, W., Frank, R., Leder, S., Joost, H. G. and Becker, W. (2000). Specificity determinants of substrate recognition by the protein kinase DYRK1A. *J. Biol. Chem.* **275**, 2431-2438.

Kaech, S., Parmar, H., Roelandse, M., Bornmann, C. and Matus, A. (2001). Cytoskeletal microdifferentiation: a mechanism for organizing morphological plasticity in dendrites. *Proc. Natl. Acad. Sci. USA* **98**, 7086-7092.

Kasai, H., Matsuzaki, M., Noguchi, J., Yasumatsu, N. and Nakahara, H. (2003). Structure-stability-function relationships of dendritic spines. *Trends Neurosci.* **26**, 360-368.

Kim, A. S., Kakalis, L. T., Abdul-Manan, N., Liu, G. A. and Rosen, M. K. (2000). Autoinhibition and activation mechanisms of the Wiskott-Aldrich syndrome protein. *Nature* **404**, 151-158.

Kim, Y., Sung, J. Y., Ceglia, I., Lee, K. W., Ahn, J. H., Halford, J. M., Kim, A. M., Kwak, S. P., Park, J. B., Ho Ryu, S. et al. (2006). Phosphorylation of WAVE1 regulates actin polymerization and dendritic spine morphology. *Nature* **442**, 814-817.

Lee, S., Lee, K., Hwang, S., Kim, S. H., Song, W. K., Park, Z. Y. and Chang, S. (2006). SPIN90/WISH interacts with PSD-95 and regulates dendritic spinogenesis via an N-WASP-independent mechanism. *EMBO J.* **25**, 4983-4995.

Liu, T., Sims, D. and Baum, B. (2009). Parallel RNAi screens across different cell lines identify generic and cell type-specific regulators of actin organization and cell morphology. *Genome Biol.* **10**, R26.

Lochhead, P. A., Sibbet, G., Morrice, N. and Cleghon, V. (2005). Activation-loop autophosphorylation is mediated by a novel transitional intermediate form of DYRKs. *Cell* **121**, 925-936.

Machesky, L. M. and Insall, R. H. (1998). Scar1 and the related Wiskott-Aldrich syndrome protein, WASP, regulate the actin cytoskeleton through the Arp2/3 complex. *Curr. Biol.* **8**, 1347-1356.

Mattila, P. K. and Lappalainen, P. (2008). Filopodia: molecular architecture and cellular functions. *Nat. Rev. Mol. Cell Biol.* **9**, 446-454.

Murakami, N., Xie, W., Lu, R. C., Chen-Hwang, M. C., Wieraszko, A. and Hwang, Y. W. (2006). Phosphorylation of amphiphysin I by minibrain kinase/dual-specificity tyrosine phosphorylation-regulated kinase, a kinase implicated in Down syndrome. *J. Biol. Chem.* **281**, 23712-23724.

Park, J., Yang, E. J., Yoon, J. H. and Chung, K. C. (2007). Dyrk1A overexpression in immortalized hippocampal cells produces the neuropathological features of Down syndrome. *Mol. Cell. Neurosci.* **36**, 270-279.

Park, J., Song, W. J. and Chung, K. C. (2009a). Function and regulation of Dyrk1A: towards understanding Down syndrome. *Cell. Mol. Life Sci.* **66**, 3235-3240.

Park, J., Oh, Y. and Chung, K. C. (2009b). Two key genes closely implicated with the neuropathological characteristics in Down syndrome: DYRK1A and RCAN1. *BMB Rep.* **42**, 6-15.

Park, J., Oh, Y., Yoo, L., Jung, M. S., Song, W. J., Lee, S. H., Seo, H. and Chung, K. C. (2010). Dyrk1A phosphorylates p53 and inhibits proliferation of embryonic neuronal cells. *J. Biol. Chem.* **285**, 31895-31906.

Prehoda, K. E., Scott, J. A., Mullins, R. D. and Lim, W. A. (2000). Integration of multiple signals through cooperative regulation of the N-WASP-Arp2/3 complex. *Science* **290**, 801-806.

Rohatgi, R., Ho, H. Y. and Kirschner, M. W. (2000). Mechanism of N-WASP activation by CDC42 and phosphatidylinositol 4,5-bisphosphate. *J. Cell Biol.* **150**, 1299-1310.

Ryoo, S. R., Jeong, H. K., Radnaabazar, C., Yoo, J. J., Cho, H. J., Lee, H. W., Kim, I. S., Cheon, Y. H., Ahn, Y. S., Chung, S. H. et al. (2007). DYRK1A-mediated hyperphosphorylation of Tau. A functional link between Down syndrome and Alzheimer disease. *J. Biol. Chem.* **282**, 34850-34857.

Ryoo, S. R., Cho, H. J., Lee, H. W., Jeong, H. K., Radnaabazar, C., Kim, Y. S., Kim, M. J., Son, M. Y., Seo, H., Chung, S. H. et al. (2008). Dual-specificity tyrosine(Y)-phosphorylation regulated kinase 1A-mediated phosphorylation of amyloid precursor protein: evidence for a functional link between Down syndrome and Alzheimer's disease. *J. Neurochem.* **104**, 1333-1344.

Scales, T. M., Lin, S., Kraus, M., Goold, R. G. and Gordon-Weeks, P. R. (2009). Nonprimed and DYRK1A-primed GSK3 beta-phosphorylation sites on MAP1B regulate microtubule dynamics in growing axons. *J. Cell Sci.* **122**, 2424-2435.

Shin, N., Lee, S., Ahn, N., Kim, S. A., Ahn, S. G., YongPark, Z. and Chang, S. (2007). Sorting nexin 9 interacts with dynamin 1 and N-WASP and coordinates synaptic vesicle endocytosis. *J. Biol. Chem.* **282**, 28939-28950.

Sitz, J. H., Tigges, M., Baumgärtel, K., Khaspekov, L. G. and Lutz, B. (2004). Dyrk1A potentiates steroid hormone-induced transcription via the chromatin remodeling factor Arip4. *Mol. Cell. Biol.* **24**, 5821-5834.

Suetsugu, S., Hattori, M., Miki, H., Tezuka, T., Yamamoto, T., Mikoshiba, K. and Takenawa, T. (2002). Sustained activation of N-WASP through phosphorylation is essential for neurite extension. *Dev. Cell* **3**, 645-658.

Takenawa, T. and Suetsugu, S. (2007). The WASP-WAVE protein network: connecting the membrane to the cytoskeleton. *Nat. Rev. Mol. Cell Biol.* **8**, 37-48.

Tatebe, H., Nakano, K., Maximo, R. and Shiozaki, K. (2008). Pom1 DYRK regulates localization of the Rga4 GAP to ensure bipolar activation of Cdc42 in fission yeast. *Curr. Biol.* **18**, 322-330.

Wegner, A. M., Nebhan, C. A., Hu, L., Majumdar, D., Meier, K. M., Weaver, A. M. and Webb, D. J. (2008). N-wasp and the arp2/3 complex are critical regulators of actin in the development of dendritic spines and synapses. *J. Biol. Chem.* **283**, 15912-15920.

Wisniewski, K. E., Laure-Kamionowska, M. and Wisniewski, H. M. (1984). Evidence of arrest of neurogenesis and synaptogenesis in brains of patients with Down's syndrome. *N. Engl. J. Med.* **311**, 1187-1188.

Yamada, H., Padilla-Parra, S., Park, S. J., Itoh, T., Chaineau, M., Monaldi, I., Cremona, O., Benfenati, F., De Camilli, P., Coppey-Moisan, M., Tramier, M., Galli, T. and Takei, K. (2009). Dynamic interaction of amphiphysin with N-WASP regulates actin assembly. *J. Biol. Chem.* **284**, 34244-34256.